JOURNAL OF PROPULSION AND POWER
Vol. 23, No. 4, July–August 2007

Flow-Control-Enabled Aggressive Turbine Transition Ducts and Engine System Analysis

R. Florea, L. Bertuccioli, and T. G. Tillman
United Technologies Research Center, East Hartford, Connecticut 06108

DOI: 10.2514/1.13488

A methodology for designing flow-control-enabled aggressive transition ducts and evaluating their system-level benefits is presented. The present methodology consists of a novel approach of coupling a parametric transition-duct geometry with a flow control model to optimize aggressive-transition-duct shapes to reduce and/or eliminate flow separations and maximize system performance. Without boundary-layer control, the flow through these aggressive transition ducts is characterized by large pressure losses due to massive flow separation, resulting in low system performance. Flow control has the potential to eliminate flow separation in these aggressive transition ducts and was included in the present study as an enabling technology. A hierarchy of high- and low-fidelity models was used to include the relevant system effects, capturing not only the performance of the transition duct itself, but also the impact of the exit flow from the transition duct on the low-pressure turbine and the engine and aircraft performance. The methodology was used to maximize range with minimum fuel burn by evaluating a system defined by families of transition-duct geometries with large radial offsets coupled with a meanline representation of a low-pressure turbine. In this example, aircraft and propulsion benefits include the elimination of a low-pressure-turbine stage, which in turn translates into significant weight savings and compactness, while maintaining or improving overall propulsion system performance. The analysis also provides a direction for future studies aimed at defining the required transition-duct radial offsets and the corresponding flow control authority levels to achieve aircraft range and total fuel-burn benefits.

Nomenclature

C_T	=	overall weight-savings coefficient (aircraft structure and nacelle)
R_M	=	low-pressure-turbine inlet meanline radius
u_τ	=	friction velocity
ΔW_{LPT}	=	low-pressure-turbine weight savings with respect to the baseline design
η_{LPT}	=	low-pressure-turbine efficiency
θ_M	=	low-pressure-turbine inlet meanline flow-path radial angle
ς	=	transition-duct total pressure loss coefficient

I. Introduction

ONE of the major advancements in jet engines is the development of high-temperature materials and cooling technology for turbine components. This technology has allowed the use of smaller cores (reduced flow and diameter) that rotate at higher, more efficient, speeds and operate at higher pressure ratios [1]. These smaller cores have emphasized the need to increase the radial offset between the low-spool turbomachinery components and the high-spool components. Conventional diffuser-design methodology indicates that to achieve good diffuser (i.e., transition duct) performance, a large radial offset would require large axial lengths. These large axial lengths would significantly reduce the weight and cost benefit of implementing a large radial offset transition duct. Shown in Fig. 1 is a typical commercial engine with the high-pressure turbine (HPT), the baseline transition duct, and the low-pressure turbine (LPT) identified.

Presented as Paper 3512 at the 3rd AIAA Flow Control Conference, San Francisco, CA, 5–8 June 2006; received 20 September 2004; revision received 12 January 2007; accepted for publication 20 January 2007. Copyright © 2007 by Razvan Florea. Published by the American Institute of Aeronautics and Astronautics, Inc., with permission. Copies of this paper may be made for personal or internal use, on condition that the copier pay the $10.00 per-copy fee to the Copyright Clearance Center, Inc., 222 Rosewood Drive, Danvers, MA 01923; include the code 0748-4658/07 $10.00 in correspondence with the CCC.

The current study addressed the optimized design of a flow-control-enabled turbine transition duct with significant radial offset compared with today's state-of-the-art commercial-engine transition ducts. A detailed feasibility (and optimization) analysis of large-radial-offset transition-duct geometries (Fig. 2) using flow control to eliminate separations is presented [1,2]. Aggressive transition ducts permit increased radial offset between the HPT and the LPT and larger annulus-area ratios across the duct. The increased radius results in more LPT tangential speed (for the same rpm), so that for the same optimum loading parameter (wheel speed squared over work), the number of stages can be reduced. Alternatively, a more aggressive transition duct can be used to trade for overall propulsion system length and weight. The increased area ratio enabled by an aggressive transition duct provides more airfoil convergence (inlet flow area over the exit flow area) in the front stages of the LPT. This in turn facilitates more favorable airfoil pressure distributions and improved performance [1]. Therefore, the aggressive transition duct can reduce the engine weight and improve the (LPT) performance and has the potential to reduce the total fuel burn for a given mission profile and/or increase the mission range [1,2].

Because flow control is such a key ingredient to the application of large-radial-offset transition ducts, it is important to realize that this study is predicated on the assumption that flow control is not a mature and robust technology and will need to be developed for this application. Although flow control was included in the numerical simulations, it was modeled as steady flow injection and scheduled at higher levels of flow than may be needed when unsteady-flow-actuation techniques are more mature. The goal was to ensure that the flow in the duct was well-behaved and the optimization was focused on transition-duct shape and flow-injection location. It was assumed that flow control authority, when applied to subsequent rig and engine tests, would be substantially less than that used in the current numerical simulations, based on a preliminary evaluation [2] and open literature results [3–5]. Current knowledge suggests that an order of magnitude or more of reduction in required flow control authority is possible with pulsed flow control ejection. These assumptions require further study and are not the subject of this paper.

The present work used numerical optimization methods coupled with a *design of experiments* [parametric computational fluid

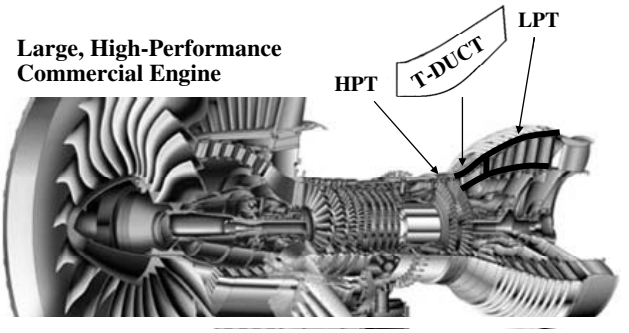

Fig. 1 Typical commercial engine with the HPT, baseline transition duct, and LPT identified.

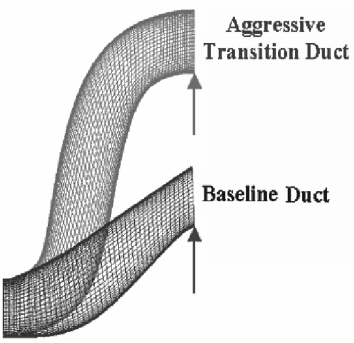

Fig. 2 Aggressive transition duct compared with baseline transition duct.

dynamics (CFD) design] of the transition-duct geometry to optimize aggressive-transition-duct shapes with flow control and reduce and/or eliminate flow separation and maximize system performance. An LPT model was included in the transition-duct optimization to capture system performance effects associated with variations in the transition-duct shape, losses, and weight savings. The LPT model consisted of a meanline LPT performance map for ranges of inlet radii and LPT inlet total pressures and temperatures from the transition-duct simulations.

Of primary importance was to evaluate what benefits in the total fuel consumption and range might be achievable with boundary-layer control technologies applied to optimized turbine transition-duct designs with large radial offsets and area ratios. A large, high-performance LPT, transition duct, and aircraft model were used as the baseline to conduct the transition-duct design study and to evaluate the resulting propulsion system benefits.

II. Methodology

The optimization process used in the present study uses numerical simulation results from a parameterized transition-duct design system and couples those results with a LPT model to obtain system efficiency. Several simplifying assumptions were made to encompass the widest range of transition-duct-shape optimization for the selected parameter space. For example, the present analysis is restricted to nominal operating conditions and steady effects (not all HPT and LPT effects are fully considered). Additionally, three-dimensional effects are neglected, in that the CFD analyses are 2-D axisymmetric with no swirl, which is an approximation of the outlet flow of the two-stage HPT used as a baseline. In the present study, the transition-duct simulations and the LPT modeling are conducted separately, and the results are connected by a methodology that corrects the transition-duct outlet-flow parameters to the nominal transition-duct/LPT system parameters at the interface. Additionally, the LPT system characteristics are modeled with a performance map to reduce the number of inner-loop optimizations of the LPT design.

The geometric parameters of the transition-duct design and the LPT flow path combined with the system-efficiency information are used to determine system-level objective functions, that is, weight, range, and fuel burn of a propulsion system, which includes the engine and the airframe. The flow modeling of the parametric transition duct, coupling corrections, and LPT meanline modeling are described next.

A. Flow Modeling of Parametric Transition Duct

A set of parameters is used to define the transition duct and the flow control injection sites. For a given duct length, exit radius, and span, eleven parameters are used to design the transition-duct shape and area distribution along the meanline. These parameters affect the radial offset, the outlet meanline flow-path angle, and the distribution of the curvature along the transition duct. The outer and inner duct walls are prescribed with an area distribution function along the meanline. The area distribution function is allowed to attain its peak before or at the outlet section and it can overshoot its exit value by up to 10%. Using the parametric definition of the transition duct and a design of experiments approach, 430 transition-duct geometries were generated to span the parametric space selected for this study. Preliminary results for calculations reported in [6] indicated that two injection slots on the upper wall are optimal to control flow separation in this class of aggressive transition ducts and that the optimal position of these injectors is dependent on duct geometry. The procedure to define the injection-slot locations is described in Sec. II.B.

The analysis and systematic exploration of the new design space was accomplished using an aerodynamic flow solver (Reynolds-averaged Navier–Stokes solver with a second-order spatial discretization and a k-ω turbulence model), a parametric transition-duct design tool, and a computer-based optimization system. The in-house aerodynamic flow code is validated for turbomachinery flow calculations and is described in [7]. The flow through the transition duct was evaluated for each parametric geometry, with and without flow injection. The parameters associated with conducting the numerical simulations are as follows:

1) The flow is assumed to be 2-D axisymmetric.

2) Fixed and uniform inflow boundary conditions were assumed. A schematic showing the inlet, exit, and wall boundary conditions is provided in Fig. 3. The duct was extended upstream such that at the location of the HPT transition-duct interface, it matches the incoming outer-casing-wall boundary layer at nominal conditions.

3) The total temperature at the inlet of each slot and the duct was fixed and uniform.

4) The inlet total pressure and temperature used in the calculations are the same for all cases.

5) The inflow swirl and pitch angles are both 0 deg relative to axial.

6) The exit static pressure was maintained constant at the hub for all cases.

7) Slip wall boundary conditions were imposed up to two cells before the injection locations along the walls of each of the slot channels. For the last two cells inside the slot channel and along the transition-duct walls, no-slip boundary conditions were applied.

8) For simplicity, the total pressure at the inlet of each slot was chosen to be 2% greater than the duct inlet total pressure and resulted in the injection of approximately 3% of the duct mass flow per slot.

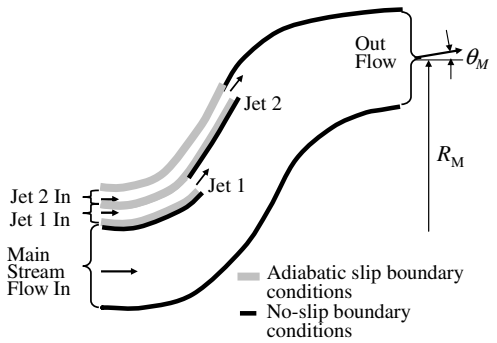

Fig. 3 Schematic representation of applied boundary conditions of transition-duct numerical model.

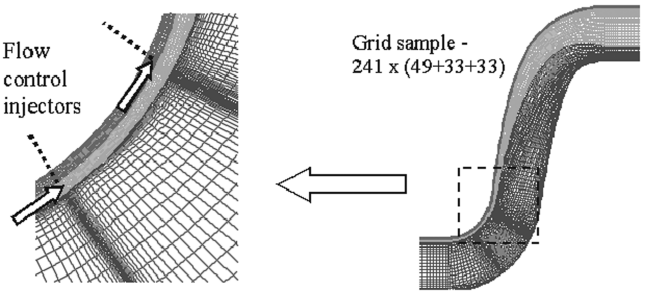

Fig. 4 Axisymmetric H-block grids are used to model the flow control injection slots and couple with the main gas path.

This total pressure was chosen to ensure a positive flow out of the injection slots and does not necessarily represent the total pressure requirement for the injected flow in an engine.

9) Simple H-block grids were used to discretize the duct flow path, with and without flow injection. A grid-refinement study was performed to determine the optimal grid size for different configurations (number of injection locations). For example, with two flow-injection slots, a $241 \times (49 + 33 + 33)$ mesh size was found to produce grid-independent results. The mesh is refined in the streamwise direction at locations near the injection points, as shown in Fig. 4.

Note that significant simplifications were made in the modeling of the injection-slot flows. In particular, slip boundary conditions were applied to the flow control walls before entry into the main gas path. The objective of the study was not to complete a detailed design of a flow control delivery system, but rather to assess the feasibility of achieving vehicle propulsion benefits by using flow control technology to open up new LPT design space. Nonetheless, the present model captures some of the main characteristics of the proposed flow control solution: namely, the slots are tangential to the duct wall and have finite thickness. However, there is zero thickness separating the jet from the mainstream flow. Further studies are required to design an effective flow control solution and this would include defining the details of the flow control delivery system, the associated pressure requirements, and the source of the bleed air.

The grid size and the k-ω turbulence model parameters were selected to be consistent with standard practice requirements, to match the turbine component predictions to experimental engine and component performance data. For instance, the grid resolution used in the present study was found to be sufficient to capture the salient features of turbine-tip-leakage flows. A grid-refinement study was completed to determine the resolution necessary to achieve convergence of the skin friction coefficient up to the separation point, within 0.5% convergence accuracy.

For each transition-duct geometry, depending on the pressure losses and on the existence and level of flow separation within the transition duct, the mass flow from the CFD simulation differed from the baseline mass flow through the LPT. Separated-flow cases correspond to high-pressure losses and unacceptable spanwise profiles and were not considered for the system-level study. For the unseparated-flow cases, the flow quantities predicted by the CFD calculations differed (slightly) from those that would have been achieved with the same geometry but the baseline mass flow. In the present study, a simple, adiabatic, "no-wall-friction" mixing model was used as a basis to correct the duct total pressure for mass flow variations in the various transition-duct simulations. This simple approach, an extension of Denton's [8] loss model, minimized the need for additional CFD simulations while maintaining the accuracy and fidelity of the original calculations for small mass flow variations. The adiabatic mixing model is based on the global conservation of mass, momentum, and energy and is applied at several locations along the transition duct. Using the CFD inflow values at duct and slot inlets (total pressure, total temperature, and mass flow), the adiabatic model predicts an ideal outlet total pressure. The outlet total pressures from the adiabatic model and the CFD simulation yield a total pressure loss coefficient. This pressure loss coefficient is then used to calculate the corrected outlet total pressure relative to an adiabatic model at the baseline inflow conditions. After the correction, for the system-level study, all unseparated-flow cases have the same baseline mass flow but slightly different duct-exit total pressures and temperatures.

One of the difficult aspects in designing an aggressive transition duct and LPT system is to ensure that the transition-duct-exit flow meets the LPT turbine inflow-quality requirements. The transition-duct-exit flow-profile distributions are key factors in the design of a high-performance LPT. A method to assess the quality of the exit total pressure and Mach number profile shapes was developed based on accepted design allowances. A spanwise (radial) Fourier decomposition was performed for each exit flow profile and "flatness" and "distortion" coefficients were determined. Constraints were imposed in this study to eliminate potential duct designs that did not satisfy the profile shape criteria. These constraints, based on established engine-design experience, captured the essential physical requirements and were used in an automated process.

B. Optimized Slot-Injection Location

To estimate the impact of flow-path shape and flow control location, preliminary calculations were completed for an aggressive transition duct with fixed exit meanline radius, 30 in. (0.762 m) relative to the 22 in. (0.559 m) baseline, and fixed exit meanline slope. Initially, transition ducts without any flow control injection slots were analyzed. Without flow control, variations in the transition-duct shape had a limited beneficial influence on the quality of the exit flow, that is, all profiles still show significant flow separation on the lower and/or upper wall of the transition duct. Next, a preliminary evaluation of flow control was completed. It was determined that at least two flow-injection locations were required to significantly diminish or eliminate the flow separation on the upper wall of the transition duct. These results indicate that even though the flow is dramatically improved with flow control, flow control by itself (without the optimization of the duct shape and slot location) may not be sufficient to eliminate flow separation and to obtain the desired flow quality at the exit of the aggressive transition duct.

In addition, a more detailed analysis is required to determine the optimal position of the injection slots to achieve transition-duct-exit flow profiles consistent with current design experience and with minimal duct losses. A wall shear-stress-driven criterion was formulated to specify the flow control jet locations. The process for locating the flow control slots requires two threshold friction velocity values, $u_{\tau 1}$ and $u_{\tau 2}$, and includes the following steps:

1) Compute the flowfield through each transition duct without flow control.

2) Determine the location of the first point at which the friction velocity drops under the threshold $u_{\tau 1}$ before separation.

3) Introduce the first flow control slot at this location.

4) Recompute the flowfield and monitor the location of the point at which the value of the friction velocity drops under the threshold $u_{\tau 2}$ before separation.

5) Repeat the process by adding a second slot at this new location.

For ten relevant geometries, the values for $u_{\tau 1}$ and $u_{\tau 2}$, were varied, and the quality assessment of the pressure and Mach number profiles at several sections downstream of the slot injections was used to determine the optimal values for the thresholds. Once the criteria are established, the selection of the locations for the flow control jets can be automated without the need for additional inner-loop optimizations.

C. LPT Meanline Analysis

Using the mass flow corrections described in Sec. II.A, all transition-duct cases with the unseparated flows correspond to the same mass flow and slightly different duct-exit total pressures and temperatures. A turbine meanline analysis was used to create a performance map of LPT designs over a range of inlet boundary conditions. The map was constructed for fixed baseline inlet boundary conditions (inlet total pressure, total temperature, and mass flow). Nine cases were considered, including three LPT inlet mean radii, $R_M = 25$ in. (0.635 m), 27.5 in. (0.699 m), and 30 in.

(0.762 m), with three inlet meanline flow-path radial angles, $\theta_M = 10$, 20, and 30 deg. To account for the variation in inflow conditions coming from the transition duct, a sensitivity analysis of the LPT efficiency for each of the nine cases was completed with respect to the total pressure and total temperature inflow values. Fixed inflow quantities and the results of the sensitivity analysis permitted a decoupled analysis of the LPT and transition-duct design. Based on a previous study [1], the improved LPT aerodynamic performance due to higher LPT radius was traded for the elimination of an LPT stage. A weight-savings analysis was performed for all nine nominal LPT cases. The weight savings is defined as the difference in weight between the five-stage LPT made possible by the aggressive transition ducts of the present study and the baseline six-stage design. The weight-savings estimates include, but are not restricted to, the weight of the rotor disks and the number of blades. Therefore, the meanline performance mapping resulted in LPT efficiency and propulsion system weight for a range of inlet radii and inlet meanline flow-path radial angles, as well as performance sensitivities to the inlet total pressure and total temperature flow conditions.

For a given turbine shape, the meanline analysis determines the pressure, temperature, flow angle, and Mach number at the entrance and exit of each row of airfoils (vane and blade). The LPT inlet total temperature, total pressure, mass flow, work, and rpm were maintained at constant values consistent with a high-performance, commercial gas turbine engine. For each of the nine aggressive-transition-duct-exit geometries (i.e., transition-duct-exit radius and radial-flow angle) the turbine meanline analysis was used to optimize the LPT design by adjusting the flow path for best performance (efficiency).

D. System-Level Analysis

System-level objective functions in the optimization process are used to assess potential candidate designs. Choosing the right system-level objective function plays a key role in the success of the flow-path design-optimization process. In the present study, an additional challenge is associated with the decoupled analysis of the transition duct (CFD) and the LPT modeling, because portions of the system-level objective functions are derived from both local and system effects. In this section, we describe the system-performance analysis, specifically, the system-level objective functions, the coupling of the transition-duct numerical flow simulations with the LPT model, and the parameters needed to conduct the analysis. System-level analyses were completed to optimize the two main objectives: maximizing aircraft range and minimizing total fuel burn.

The current study attempts an optimization of the transition duct by conducting a design of experiments; a large number of transition-duct designs were analyzed over a selected range of transition-duct design space. The results of the transition-duct simulations were used in conjunction with the LPT performance-map model to calculate the range and fuel-burn benefits. An additional benefit of the decoupled approach is that the same design of experiments (transition-duct simulations) can be used for a variety of optimizations, including increasing range and reducing fuel burn.

The transition-duct results from the numerical simulations are coupled to the LPT analysis through the transfer of parameters for each transition-duct shape analyzed. The flow through the transition duct is defined by the total pressure losses and by the flatness and distortion measures of the quality of the exit total pressure and Mach number profile shapes at the interface between the transition duct and the LPT. The duct total pressure loss coefficient is defined as the ratio between the mass-averaged HPT transition-duct interface and exit total pressure quantities of the transition duct. A new LPT design is defined by its weight savings ΔW_{LPT} with respect to baseline design and efficiency η_{LPT}.

Several parameters are calculated outside the transition duct and meanline analyses, including an LPT exit-guide-vane (EGV) total pressure loss and the weight impact of the LPT system on the aircraft structure and nacelle weights. The EGV pressure losses depend on the LPT exit flow parameters that are provided by the meanline analysis, exit Mach number, and exit swirl angle. In addition, a reduction in LPT weight caused by a reduction in the number of stages results in a commensurate weight reduction in the aircraft propulsion system support structure. This additional weight-performance parameter is calculated using the output from the LPT meanline analysis and is included as part of the overall system performance. It compensates for any additional hardware associated with flow-injection delivery. The total weight savings is estimated as

$$\Delta W_T = (1 + C_T)\Delta W_{\mathrm{LPT}}$$

Based on engine-design experience, C_T was estimated to be 0.4. The benefits considered in the present system-level study are not by any means all-inclusive. For example, not considered here is the fact that a shorter LPT system can translate into reduced internal flow-path losses and nacelle drag.

Two global system-level objective functions are considered in the present study: range R and total fuel burn F. The two system-level objective functions to be optimized are expressed as a function of the bleed mass flow, transition-duct pressure loss coefficient, engine weight, LPT efficiency, and EGV pressure loss.

III. Results of System-Level Analysis

Using the parametric definition of the transition duct, including the slot-injection locations, 430 transition-duct geometries were generated to span the parametric space selected for this study. The cases considered include three LPT inlet mean radii, $R_M = 25$ in. (0.635 m), 27.5 in. (0.699 m), and 30 in. (0.762 m), with three inflow meanline flow-path radial angles, $\theta_M = 10$, 20 and 30 deg. Figure 5 shows the exit total pressure profiles for all of the transition-duct geometries in gray, with those that show no flow separation and satisfy both the pressure and Mach number profile distortion and flatness criteria highlighted in black. Note that the total pressure was normalized by its value at the HPT transition-duct interface plane and not the uniform computational inlet-plane total pressure. Although unseparated-flow cases exist for all three meanline radii, only the transition ducts with an exit meanline radius of 25 in. (0.635 m) satisfy the total pressure and Mach number profile requirements. In general, the first jet injection delays separation, whereas the second one tries to eliminate separation completely. In addition, an optimal transition-duct wall curvature allows the first jet to penetrate the boundary layer and impinge on the core flow. The overall effect of the combined jet-injection locations and wall curvature is a relatively uniform total pressure exit profile, as shown for the cases highlighted in black in Fig. 5.

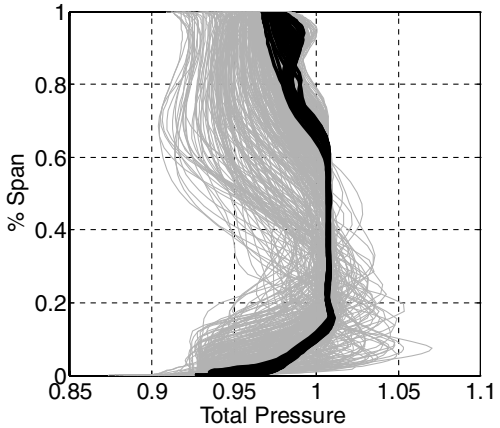

Fig. 5 Transition-duct-exit total pressure profiles (normalized by HPT transition-duct interface-plane total pressure). Marked with thick lines are the unseparated-flow cases that satisfy the total pressure and Mach number flatness and distortion restrictions.

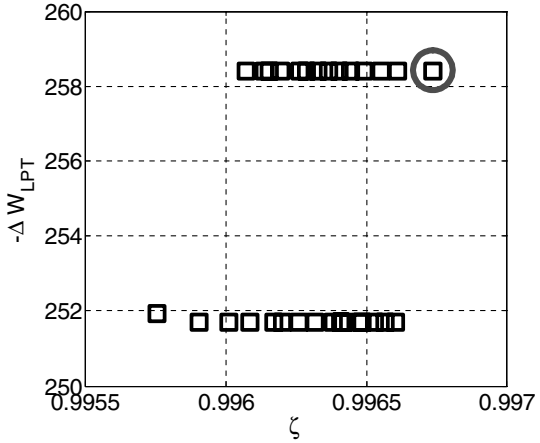

Fig. 6 System-level objective functions: ς and ΔW_{LPT} are evaluated for the unseparated flows with optimum shape profiles (Sec. III.A). All cases correspond to a meanline radius $R_M = 25$ in. (0.635 m) and LPT efficiencies around $\eta_{\mathrm{LPT}} = 0.917$. All LPTs are designed for maximum efficiency. The optimum case (AR009), marked with a ring, corresponds to $\theta_M = 10$ deg, $\varsigma = 0.997$, and $\Delta W_{\mathrm{LPT}} = -258$ kg.

A. Transition-Duct and LPT System Optimization

Initially, a partial optimization problem is carried out. For each LPT with a given inlet meanline radius and angle, the solution of the LPT design for maximum range is computed and the system benefits are determined.

The turbine meanline performance mapping provides most of the LPT system performance information directly, including the overall LPT configuration (number of stages, number of airfoils, hub and tip radii for each stage, and LPT length), total LPT weight savings W_{LPT}, LPT system losses, and efficiency η_{LPT}. Low-pressure-turbine performance information was calculated for each transition-duct numerical simulation. The duct's outlet pressure and temperature, corrected for mass flow variations from differences in transition-duct loss, were used as input to the LPT performance map for each of the three outlet radii considered. LPT performance parameters (i.e., efficiency, flow-path definition, and exit-guide-vane loss) were determined with the LPT performance map and the previously described sensitivity analysis for total pressure and temperature.

The system-level objective functions that describe the system are the transition-duct loss coefficient ς, the LPT efficiency η_{LPT}, and the transition-duct and LPT weight savings ΔW_{LPT} (Fig. 6). These objective functions were evaluated for all the transition duct/LPT systems that satisfied the flow-profile constraints for the LPT inlet mean radius case of $R_M = 25$ in. (0.635 m). Analyses for the 27.5-in. (0.699-m) and 30-in. (0.762-m) exit radii cases will be shown in subsequent sections. The optimum transition duct/LPT system that satisfied the objective functions and the profile constraints is depicted as AR009 in our notation. The case is defined by the parameters $R_M = 25$ in. (0.635 m), $\theta_M = 10$ deg, $\varsigma = 0.997$, $\Delta W_{\mathrm{LPT}} = -258$ kg, and $\eta_{\mathrm{LPT}} = 0.919$. The total pressure and Mach number field distributions for this case are shown in Fig. 7.

B. System-Level Benefits

This section describes the system-level benefits of transition-duct designs with medium and large radial offsets (27.5- and 30-in. exit radii). In the present study, the injection flow in the numerical simulations was assumed to be ~3% of the core mass flow per injection slot. This large mass fraction was not optimized, but rather was chosen to ensure that in our automated process, a potentially viable geometry was not rejected due to insufficient flow control authority. It is implied that for the designs that satisfy the flow-quality metrics, the flow control authority will be minimized and that unsteady flow actuation will be evaluated to further reduce the flow control requirements as part of a more detailed design process. Some of the possible actuation solutions were described and evaluated in [2]. System-level benefits of the overall propulsion/aircraft system were evaluated using existing mission-trade factors for a large commercial aircraft and a large, high-performance, commercial engine propulsion system [6].

Recall that for all the transition-duct cases presented in the previous subsection, only the transition ducts with an exit meanline radius of 25 in. (0.635 m) satisfy the total pressure and Mach number profile requirements. The authors suggest that significant improvements in transition-duct performance (in particular, exit flow-quality profiles) could be achieved using a higher-fidelity analysis with more detailed geometric parameterization. The assumption that significant improvements can be achieved implies that additional aggressive-transition-duct design shapes may become feasible if more detailed shape definitions are used. To achieve good designs for aggressive transition ducts with large radial offsets, the threshold imposed by the flow-quality metrics may also need to be relaxed during the initial global optimization and reapplied later in a final high-fidelity optimization step. For example, the flow-quality metrics that define the flatness and smoothness of the exit pressure and Mach number profiles may be set aside for the initial global optimization, requiring only that the flow does not separate in the transition duct on either the lower or the upper walls. Subsequently, the flow control authority could be adjusted to improve the profile flatness as needed. Cases with these relaxed profile constraints are considered in this section.

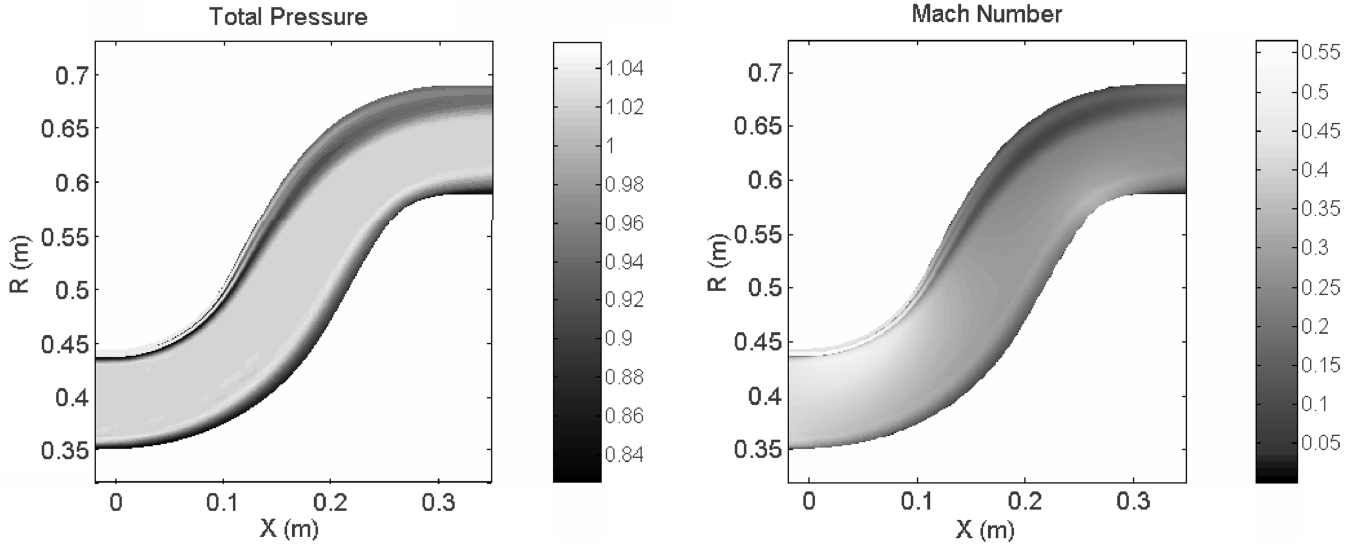

Fig. 7 Total pressure (normalized by HPT-transition-duct interface plane total pressure) and Mach number fields for the selected case (AR009); $R_M = 25$ in. (0.635 m), $\theta_M = 10$ deg, $\varsigma = 0.997$, $\Delta W_{\mathrm{LPT}} = -258$ kg, and $\eta_{\mathrm{LPT}} = 0.919$.

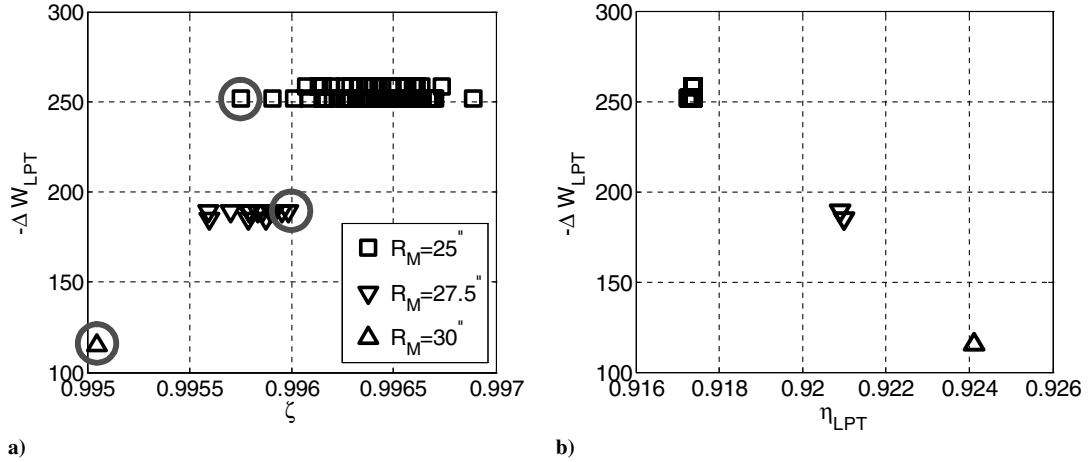

Fig. 8 System-level objective functions are evaluated for unseparated flows (Sec. III.B): a) ς and ΔW_{LPT} and b) η_{LPT} and ΔW_{LPT}. All LPTs are designed for minimum fuel burn and all radii are considered. The lowest fuel-burn cases are indicated with a ring.

Performance parameters ζ, η_{LPT}, and ΔW_{LPT} were evaluated for transition ducts with unseparated flows and varying exit radii. In the range and fuel analysis of the present study, the steady mass flow bleed was replaced with unsteady flow actuation (at a mean level of 0.5% of the total mass flow through the transition duct) to minimize the flow authority and reduce the negative impact on the engine performance. Such challenging flow-actuation designs would require further detailed unsteady and three-dimensional analyses and test evaluation. However, the requirements for these new designs are consistent with the current knowledge that suggests that an order of magnitude or more of reduction in required flow control authority is possible with pulsed flow control injection [3–5].

All LPTs were designed for minimum fuel burn [6]. To better understand the effects of the aggressive-transition-duct design on the mission-level benefits, the transition-duct losses, the LPT efficiency, and the LPT weight savings for all of the radii are shown in Fig. 8. Note that all of the unseparated cases for each radius are effectively indistinguishable in terms of transition-duct total pressure loss coefficient (though not necessarily profile flatness). This point is underscored by the fact that the LPT efficiency predictions are tightly bunched for each radius. The fuel and range benefits are shown in Fig. 9. The performance of the baseline, six-stage LPT, with a 22-in. (0.559-m) LPT inlet mean radius represents the origin. Even though the use of a less aggressive HPT-LPT radial offset ($R_M = 25$ in.) provides dramatically improved propulsion system weight reduction, the higher efficiencies associated with the larger offsets are not realized in this region of design space. The weight reduction achieved at this exit-transition-duct radius translates into a significant 0.61% improvement in range. However, no substantial benefit in fuel burn is achieved.

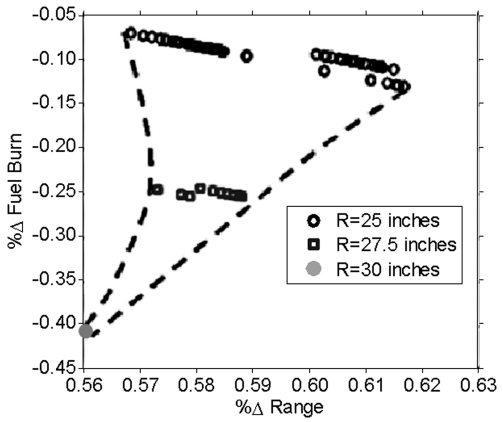

Fig. 9 Analysis of range or fuel-burn variation for unseparated-flow cases. LPT designs are optimized for minimum fuel burn and all radii are considered.

Significant improvements in range and fuel benefits are observed at larger radii when compared with $R_M = 25$ in. (0.635 m). Compared with the baseline, the fuel burn is reduced by 0.25% for $R_M = 27.5$ in. (0.699 m) and 0.4% for $R_M = 30$ in. (0.762 m). Cases with these larger exit radii achieve significantly higher LPT efficiencies and may thus prove attractive at a system level, if additional shape refinement can sufficiently improve their duct-exit flow quality. The benefits in range are around 0.59 to 0.56%, for which the lower values correspond to larger exit radii. The figure also suggests that at larger radii, robust designs are more challenging to achieve. Details of this analysis [6] (not shown here) identify that the two most significant contributions to fuel burn and range variation are the increase in LPT efficiency and the engine weight reduction.

IV. Conclusions

A novel methodology for designing flow-control-enabled aggressive turbine transition ducts coupled with shape optimization was presented. The flow through aggressive transition ducts with large radial offsets without flow control is characterized by large pressure losses due to massive flow separation and, therefore, contributes to poor system performance. Flow control was included in the present study as an enabling technology to eliminate flow separation in these aggressive transition ducts. The most relevant system effects were included, capturing not only the performance of the transition duct itself, but also the impact of the transition-duct-exit geometry and resulting flow on the LPT and the entire engine and aircraft system.

The system-level study was completed by choosing transition-duct design cases that satisfied either the exit flow-quality constraints or the weaker condition of only unseparated flows and showed promise by having higher system-level benefits. The range and fuel burn for the selected cases were computed assuming a system with a five-stage LPT and compared with the baseline six-stage LPT turbine system. The study showed that range and fuel-burn benefits depend on the radial offset of the transition duct. Indeed, a range benefit of approximately 0.6% may be realized through application of aggressive transition ducts with optimized flow control technologies that primarily result in system weight reductions through a reduction in the LPT stage count. It was also concluded that for a fixed mission profile, the transition duct/LPT system could be optimized to reduce the total fuel burn by 0.4% by increasing the radial offset.

Based on the present study, it is recommended that future work should focus on reducing required flow control authority and increasing flow control effectiveness, including exit flow-quality profiles. Recent published studies using vortex-generator-jet technology have demonstrated flow separation control on low Reynolds number airfoil blading; however, more work is needed to fully investigate the design space and verify these preliminary findings for application in turbine transition ducts.

In summary, this study shows that when flow control is coupled with duct-shape optimization, separation in aggressive transition ducts can be eliminated. The projected aircraft and propulsion benefits are promising: namely, the elimination of an LPT stage, which in turn translates in to significant weight savings and compactness, while maintaining or improving overall propulsion system efficiency.

Acknowledgments

This work was funded by the NASA John H. Glenn Research Center at Lewis Field, as part of Task 19 of the Ultra Efficient Engine Technology (UEET) Program. The NASA Task Manager and Technical Monitor was Vithal Dalsania, and the Pratt & Whitney Program Manager was John Leogrande. Special thanks are due to Dochul Choi, Duane McCormick, and Brian Wake of United Technologies Research Center and John Adamczyk of NASA John H. Glenn Research Center for their technical assistance in the areas of computational fluid dynamics and flow control technology and to Francis R. Price, Rajendra Agrawal, Joel H. Wagner, and Robert Kline at Pratt & Whitney for their technical assistance in the area of transition-duct and low-pressure-turbine design.

References

[1] Lord, W. K., MacMartin, D. G., and Tillman, T. G., "Flow Control Opportunities in Gas Turbine Engines," AIAA Fluids 2000 Conference, Denver, CO, AIAA Paper 2000-2234, 2000.

[2] Tillman, G., Lin, R., Ibrahim, Z., Bertuccioli, L., Florea, R., Nedungadi, A., Prasad, A., Patterson, R., Wake, B., Wagner, J., Price, D., Miller, J., and Magge, S., "Flow Control for Aggressive Turbine Transition Ducts and High-Lift Airfoils," United Technologies Research Center Rept. R00-4.100.0263-2, East Hartford, CT, Dec. 2000.

[3] Wygnanski, I., "Method and Apparatus for Delaying Separation of Flow from a Solid Surface," U.S. Patent 5,209,438, filed 1993.

[4] McCormick, D. C., "Boundary Layer Separation Control with Directed Synthetic Jets," AIAA 38th Aerospace Sciences Meeting, Reno, NV, AIAA Paper 2000-0519, 2000.

[5] Bons, J. P., Sondergaard, R., and Rivir, R. B., "Turbine Separation Control using Pulsed Vortex Generator Jets," TURBOEX-PO 2000: International Gas Turbine Conference, Munich, Germany, American Society of Mechanical Engineers Paper 2000-GT-0262, 2000.

[6] Florea, R., Bertuccioli, L., Lin, R., Tillman, T. G., and Wagner, J. H., "Parametric Design of Turbine Transition Ducts Using Flow Control," Pratt & Whitney, Task Order 19, NASA Contract NAS3-98005, East Hartford, CT, Feb. 2003.

[7] Davis, R. L., Ni, R. H., and Carter, J. E., "Cascade Viscous Flow Analysis Using the Navier-Stokes Equations," *Journal of Propulsion and Power*, Vol. 3, No. 5, 1987, pp. 406–414.

[8] Denton, J. D., "Loss Mechanism in Turbomachines," *Journal of Turbomachinery*, Vol. 115, Oct. 1993, pp. 621–656.

L. Xu
Associate Editor